A Reformulated General Thermal-Field-Photoemission Theory

and Application to Characterization of Compound Emitters

K. L. Jensen

[1] Code 6362, MSTD, NRL, Washington DC

7^{th} IVEW & 13^{th} IVeSC (May 26 - 29, 2020)
Workshop/Conference virtual event via Internet
Monday, May 26 @ 4 PM (GMT+2)

ACKNOWLEDGEMENTS: A. Shabaev, S. Lambrakos, M. McDonald (NRL); D. Finkenstadt (USNA); D. A. Shiffler (AFRL); N. A. Moody (LANL); J. J. Petillo (Leidos); O. Chubenko (ASU)

Sections Outline

History: TF Emission from a Tungsten Tip

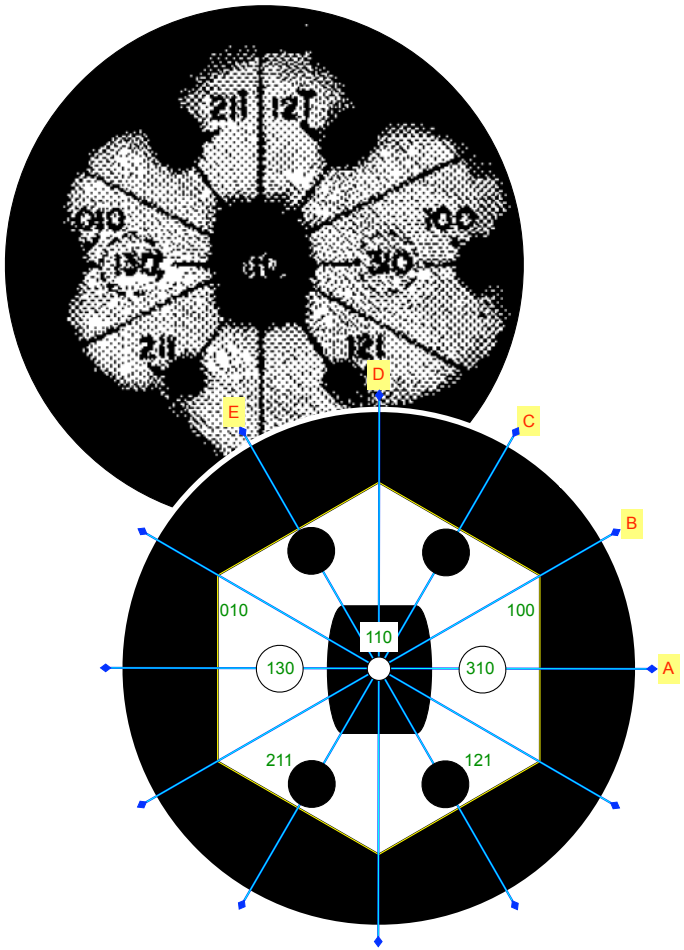

W.P. Dyke, et al. JAP25, 106, 1954

Dyke, Barbour, Martin, Trolan. *T-F Emission: Exp. Measurement of the Average Electron Current Density from W.*" Phys Rev 99, 1192, 1955

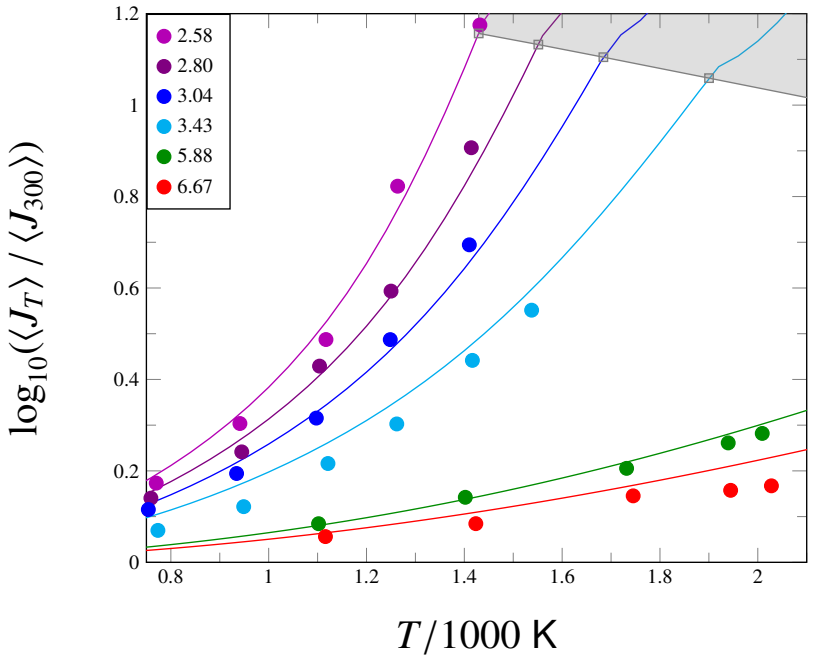

- Dyke *et al.*: as $F = q|\mathcal{E}|$ decreased, average $J(F,T)$ over surface (left) compared to $J(F, 300K)$, showed strong T-dependence
- FE sources can run **hot** at high J; TE sources can have protrusions. Breakdown sites are a combination of both.
- $10^{1.2} = 16\times$ is a substantial increase in current!
- Question: rapid way to predict $J(F,T)$ from a complex geometry?

History: TF Emission from a Barium Dispenser Cathode

Current Vs. Voltage $I(V)$:

- RLD-Like:

$$R \equiv \ln\left[\frac{I(V)}{I(V_o)}\right] \sim B\sqrt{V} - B\sqrt{V_o}$$

- FN-Like ($p = 2$)

$$R' \equiv \ln\left(\frac{I(V)}{V^p} \cdot \frac{V_o^p}{I(V_o)}\right) \sim \frac{B'}{V_o} - \frac{B'}{V}$$

For a sharp W tip:

$p \to 2 - \nu$ with $\nu \sim 0.773$

Geittner, Gärtner, and Raasch.
Low temperature properties of Ba-dispenser cathodes."
J. Vac. Sci. Technol. B **18**, 997 (2000)

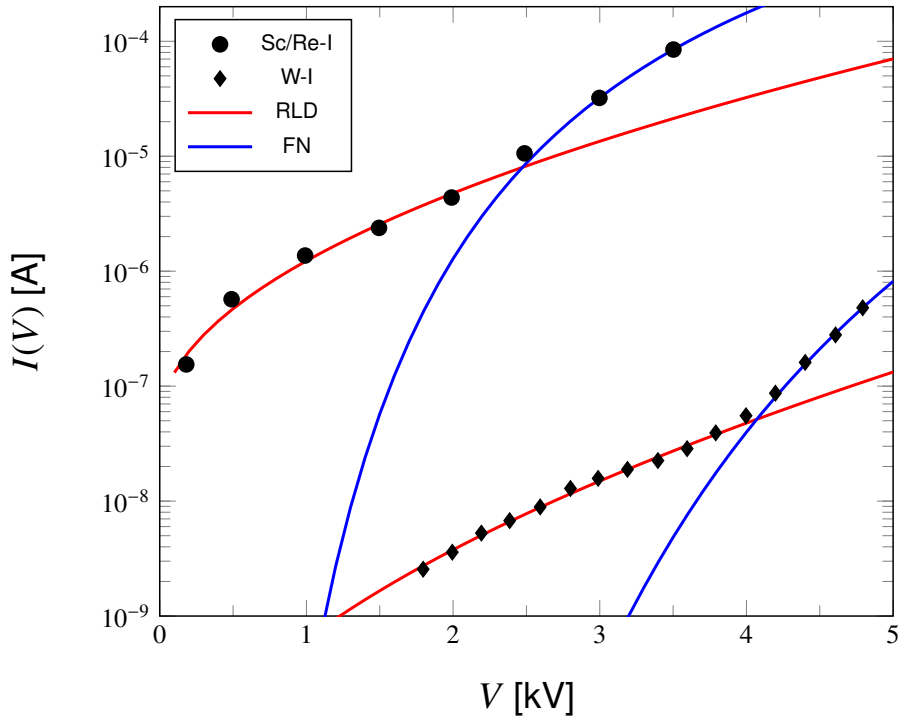

"The curves impressively demonstrate the superior emission properties of the "Sc"/Re-I cathodes (lower $e \cdot \Phi$). Compared to a pure W-I cathode, an emission gain of nearly four orders of magnitude is obtained. Moreover, superimposed to the thermionic emission both cathodes clearly show remarkable contributions by field emission..."

Units: "Though this be madness, yet there is a method in't." †

Image Charge Barrier: Defines F and Q

$$U(x) = \mu + \Phi - q|\mathcal{E}|x - \frac{q^2}{16\pi\varepsilon_0 x} \equiv \mu + \Phi - Fx - \frac{Q}{x} \quad (1)$$

Max of $U(x)$ defines ϕ

$$\partial_x U(x_o) = 0 \leftrightarrow x_o = \sqrt{Q/F} \quad (2)$$

$$\phi \equiv \Phi - \sqrt{4QF} \quad (3)$$

- F is a force; U is an energy.
- Schottky barrier lowering factor: $y(\mu) = \sqrt{4QF}/\Phi$
- Phrasing: 'Field" and "field-like" used for quantities dependent upon F.

$\alpha = \frac{q^2}{4\pi\varepsilon_o\hbar c}$ and [nefq] = nm, eV, fs, q = 1

Symbol	*Definition*	*Value*
q	unit charge	q
$\hbar$	Planck	0.658212 eV-fs
c	speed of light	299.792 nm/fs
m	e^- rest mass	510999 eV/c^2
k_B	Boltzmann	(1/11604.5) eV/K
a_o	Bohr Radius	0.052918 nm
R_y	Rydberg Energy	13.6057 eV
α	Fine Structure	1/137.036
Q	$\alpha\hbar c/4$	0.36 eV-nm

Quantity	*MKSA unit*	*Relation*
Length	meter	10^9 nm
Time	second	10^{15} fs
Energy	Joule	6.2415×10^{18} eV
Charge	Coulomb	6.2415×10^{18} q
Current	Amp	6241.5 q/fs
Power	Watt	6241.5 eV/fs
Field	GV/m	1 eV/(q-nm)
Force $F = q\mathcal{E}$	q GV/m	1 eV/nm
Pot. Energy $V = q\varphi$	q Volt	1 eV

† William Shakespeare, *The Tragedy of Hamlet, Prince of Denmark*, Act II Scene ii Lines 203-204

The Canonical Equations

Thermal: Richardson-Laue-Dushman

C. Herring, M. Nichols, Rev. Mod. Phys. 21, 185 (1949).

$$J_{RLD}(T) = A_{RLD} T^2 \exp\left(-\frac{\phi}{k_B T}\right) \quad (4)$$

Field: Fowler Nordheim

E.L. Murphy, R.H. Good, Phys Rev 102, 1464 (1956).

$$J_{FN}(F) = \frac{A_{FN}}{t(y)^2} F^2 \exp\left(-v(y)\frac{B_{FN}\Phi^{3/2}}{F}\right) \quad (5)$$

Photo: Fowler-DuBridge

L.A. DuBridge, Phys. Rev. 43, 0727 (1933).

$$QE \equiv \frac{\hbar\omega}{q}\left(\frac{J}{I_\omega}\right) \propto (\hbar\omega - \phi)^2 \quad (6)$$

Secondary: Baroody

E.M. Baroody, Phys. Rev. **78**, 780 (1950)

$$\delta(E_o) = BE_o e^{-\lambda} \int_0^1 \exp\left(\lambda s^2\right) ds \quad (7)$$

Space Charge: Child-Langmuir

I. Langmuir, Phys. Rev. **2**, 450 (1913).

$$J_{CL}(\varphi_a) = \frac{4\varepsilon_0}{9D^2}\left(\frac{2q}{m}\right)^{1/2} \varphi_a^{3/2} \quad (8)$$

Φ = Work Function; T = Temperature; $F = q\mathcal{E}$;
$\hbar\omega$ = Photon energy; I_ω = laser intensity;
E_o = Primary electron beam energy;
λ = energy loss per unit length
D = anode-cathode gap; φ_a = anode potential

Equations follow from J evaluation

General Current Density I

- For eigenstates $\psi_k(x)$:

$$j_k(x,t) = \frac{\hbar}{2mi}\left\{{\psi_k}^\dagger \partial_x \psi_k - \psi_k \partial_x {\psi_k}^\dagger\right\}$$

- Transmission probability: ratio of j_k

$$D(k) = \frac{j_{trans}(k)}{j_{incident}(k)} \qquad (9)$$

Rectangular barrier: $D(k) = |t(k)|^2$

Supply function from FD Distribution

$$\beta_T = \frac{1}{k_B T}$$

$$E = \frac{\hbar^2}{2m}\left(k_x^2 + k_\perp^2\right) = E_x + E_\perp$$

$$f(k_x) = \frac{2}{2\pi^2}\int_0^\infty \frac{2\pi k_\perp dk_\perp}{1 + e^{\beta_T(E-\mu)}} = \frac{m}{\pi\beta_T\hbar^2}\ln\left[1 + e^{\beta_T(\mu - E_x)}\right] \qquad (10)$$

Tsu-Esaki-like (1D) Current Density Relation with $E(k) = \hbar^2 k^2/2m$

$$J(F,T) = q\rho\frac{\hbar\langle k\rangle}{m} = \frac{q}{2\pi}\int_0^\infty \frac{\hbar k}{m} D(k) f(k)\, dk = \frac{q}{2\pi\hbar}\int_0^\infty D(E) f(E)\, dE \qquad (11)$$

General Current Density II

Barrier Height $V_o = \hbar^2 k_o^2/2m$, width L

$$\frac{1}{D_{rec}(k)} \equiv 1 + \frac{k_o^4 \sinh^2\left(L\sqrt{k_o^2 - k^2}\right)}{4k^2(k_o^2 - k^2)} \qquad (12)$$

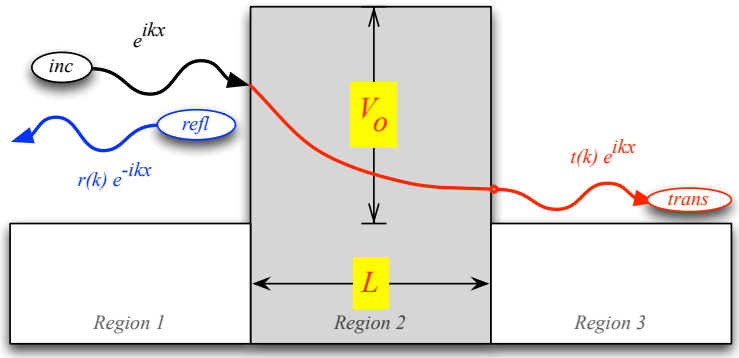

- Gamow Factor (*aka* "WKB")

$$\theta(k) = 2L\sqrt{k_o^2 - k^2}$$
$$\rightarrow 2\int_{x_-}^{x_+} k(x)\,dx \qquad (13)$$

- Kemble form of D(k):

$$D(k) \approx \frac{1}{\{1 + \exp[\theta(k)]\}} \qquad (14)$$

- $D(k_o) \neq 1/2$; $D(k > k_o)$ oscillates.

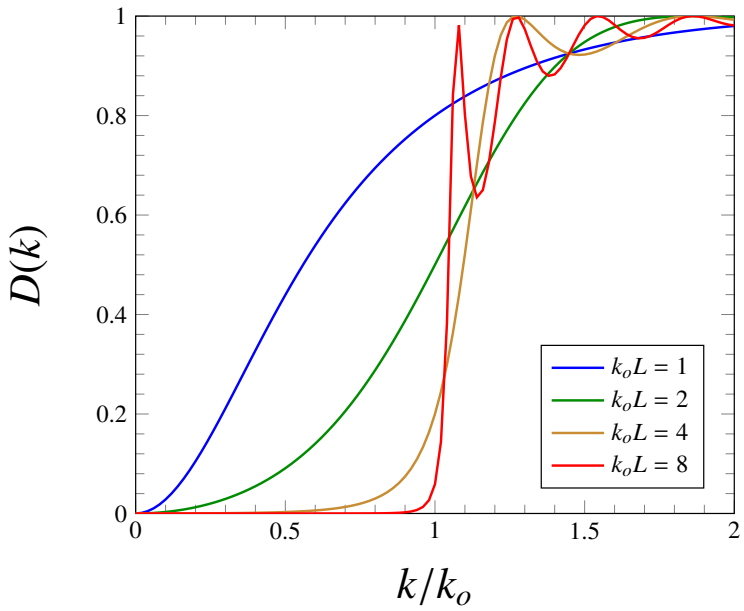

General Current Density III

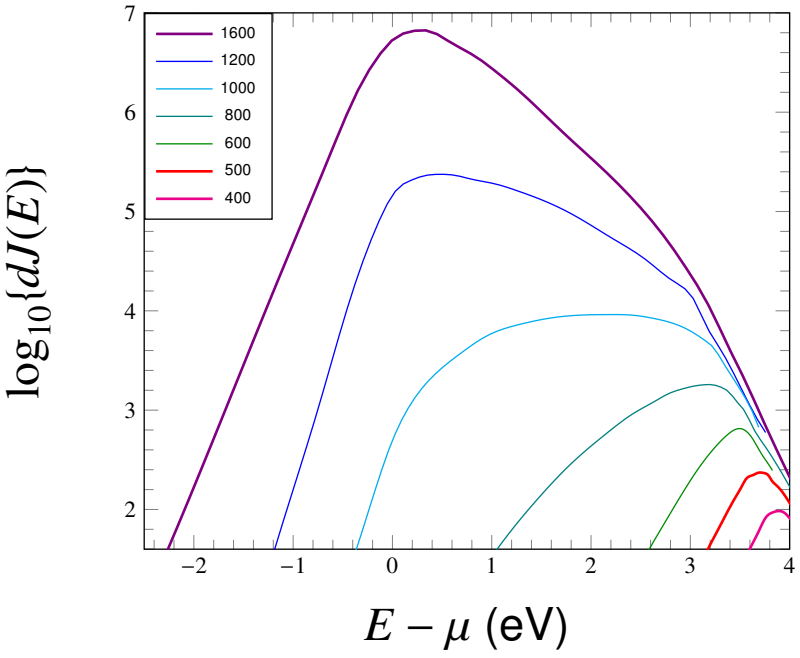

Measured Total E Distributions: Voltage increased from 500 V (1.1 GV/m) to 1600 V (3.5 GV/m) E_m moves from $\mu+\phi$ to μ.

- J.W. Gadzuk, and E.W. Plummer. "*Energy Distributions for Thermal Field Emission.*" Phys. Rev. B, **3(7)**, 2125, 1971.
- See also: M.J. Fransen, T.H.L. Van Rooy, *et al.*, *Electron Emission Physics: Advances in Imaging and Electron Physics Vol III*, ed. P. Hawkes 1999).

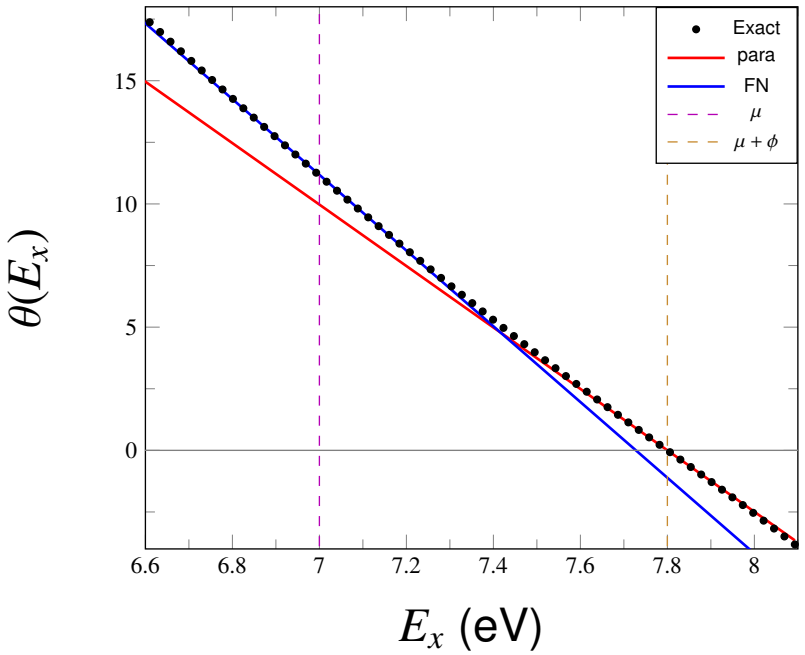

Exact $\theta(E_x)$ compared to linear approximations using $\beta_F(\mu)$ and $\beta_F(\mu+\phi)$ used in oGTF equation.

- $T = 850$ K, $F = 1$ eV/nm
- $\mu = 7$ eV, $\Phi = 2$ eV
- Gray $\theta = 0$ (horizontal); $E = \mu, \mu+\phi$ (vertical)
- $\theta(E)$ is well approximated by a cubic polynomial

General Current Density IV

Insert $f(E)$ + Kemble $D(E)$ into Tsu-Esaki

$$J(F,T) = \frac{qm}{2\pi^2\beta_T\hbar^2}\int_0^\infty \frac{\ln\{1+\exp[\beta_T(\mu-E)]\}}{1+\exp(\theta(E))}dE \approx A_{RLD}T^2N\left[\frac{\beta_T}{\beta_F(E_m)},\theta(E_m)\right] \quad (15)$$

$N(n,s): \theta(E) \rightarrow \theta(E_m) + \beta_F(E_m)\,(E_m - E)$, $\beta_T = 1/k_BT$ & $\beta_F \rightarrow$ E-slope factors

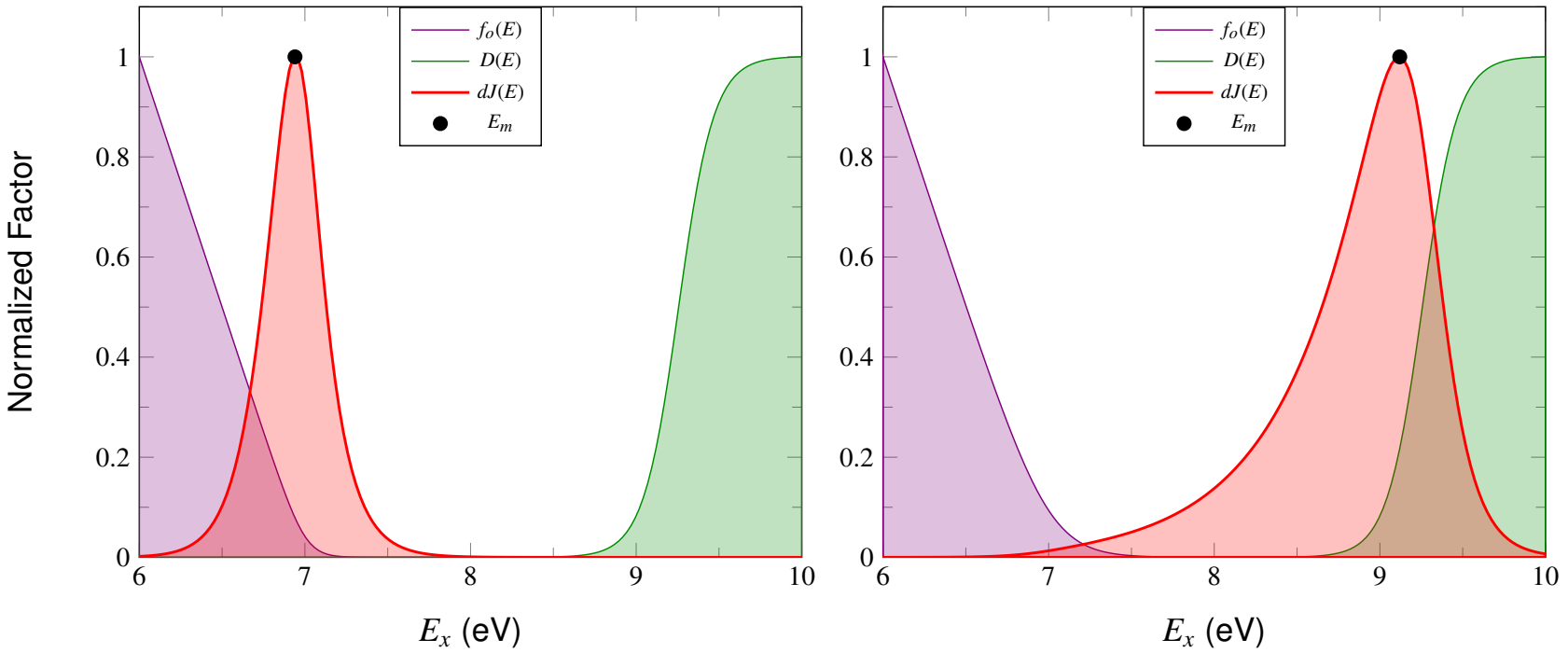

Factors: $\mu = 7$ eV, $\Phi = 4.5$ eV, $F = 2.7$ eV/nm. (*left*) $T = 700$ K; (*right*) $T = 1570$ K

Original General Thermal-Field-Photoemission (oGTFP) I

N(n,s) Approximation

$$N(n,s) \approx e^{-s} n^2 \Sigma\left(\frac{1}{n}\right) + e^{-ns}\Sigma(n) \tag{16}$$

$$N(1,s) = (s+1)e^{-s} \tag{17}$$

$$\Sigma(x) \approx \frac{1+x^2}{1-x^2} - 0.36\,x^2 - 0.106\,x^4 \tag{18}$$

Define functions $n(F,T)$ and $s(F,T)$ by

- (F-like): $T < T_{min}$: $E_m \to \mu$
- (T-like): $T > T_{max}$: $E_m \to \mu + \phi$
- (TF-like): Otherwise: $\beta_T = \beta_F(E_m)$

Energy Slope and Barrier Reduction

- Thermal $\to \beta_T = 1/k_B T$
- Field $\to \beta_F(E) \equiv -\partial_E \theta(E)$
- $y(\mu) = \sqrt{4QF}/\Phi$

Gamow Factor $\theta(E)$ rewritten:

$$\begin{aligned}\theta(E) &\equiv 2\frac{\sqrt{2m}}{\hbar}\int_{x_-}^{x_+}\sqrt{U(x)-E}\,dx \\ &\approx \theta(E_m) + \beta_F(E_m)(E_m - E)\end{aligned} \tag{19}$$

Special Cases for image charge $U(x)$ using Elliptical Integral Functions $v(y)$ and $t(y)$

$$\begin{aligned}\theta(\mu) &= \frac{4}{3\hbar F}\sqrt{2m\Phi^3}\,v[y(\mu)] \\ \theta(\mu+\phi) &= 0 \\ \beta_F(\mu) &= \frac{2}{\hbar F}\sqrt{2m\Phi}\,t[y(\mu)] \equiv \frac{1}{k_B T_{min}} \\ \beta_F(\mu+\phi) &= \frac{\pi}{\hbar F}\sqrt{m\Phi}\,\sqrt{y(\mu)} \equiv \frac{1}{k_B T_{max}}\end{aligned} \tag{20}$$

Extension to Photoemission:

$$\begin{aligned}\theta(E_m) &\to \theta(E_m + \hbar\omega) \\ N(n,s) &\to N(n,-s)\end{aligned} \tag{21}$$

Original General Thermal-Field-Photoemission (oGTFP) II

General Thermal-Field current density $J_{GTF}(F,T)$

$$J_{GTF}(F,T) = \begin{cases} n^{-2}J_F + J_T & (n<1) \\ J_F + n^2 J_T & (n>1) \end{cases} \tag{22}$$

The two current densities J_F and J_T are defined by

$$J_F = A_{RLD}(k_B\beta_F)^{-2}\Sigma\left(\frac{\beta_F}{\beta_T}\right)\exp\left[-\beta_F(E_o-\mu)\right] \qquad (n\to\infty, J_F\to J_{FN}) \tag{23}$$

$$J_T = A_{RLD}(k_B\beta_T)^{-2}\Sigma\left(\frac{\beta_T}{\beta_F}\right)\exp\left[-\beta_T(E_o-\mu)\right] \qquad (n\to 0, J_T\to J_{RLD}) \tag{24}$$

Generalized Photoemission current density $J_P(F,T)\propto QE\, I_\omega$

$$J_P \propto (\hbar\omega-\phi)^2 + \frac{\pi^2}{3}\left(\beta_T^{-2}+\beta_F^{-2}\right) \qquad (n^2\ll 1, J_P\to J_{FD}) \tag{25}$$

Remember: $n=\frac{\beta_T}{\beta_F}$, $\phi=\Phi-\sqrt{4QF}$, $\Sigma(n)=\frac{1+n^2}{1-n^2}$, $\Sigma(n^{-1})=\frac{n^2+1}{n^2-1}$

Original General Thermal-Field-Photoemission (oGTFP) III

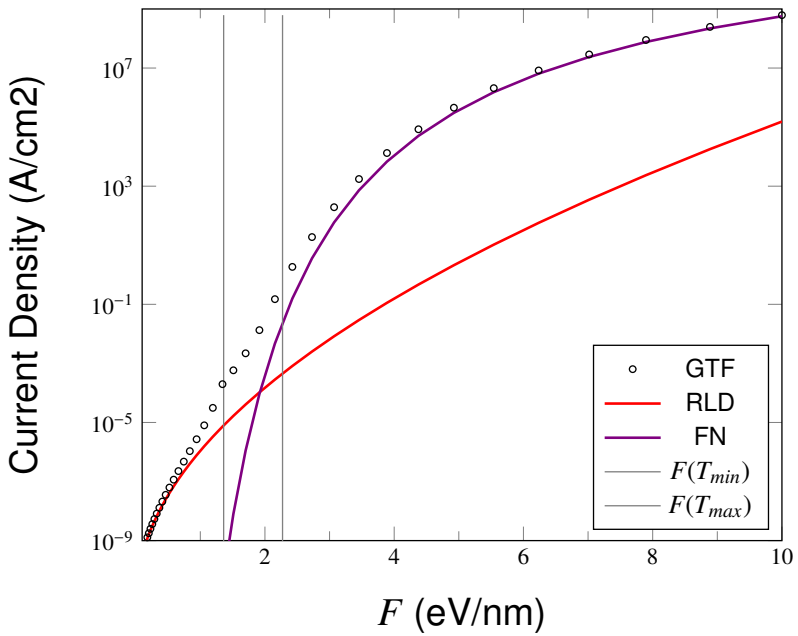

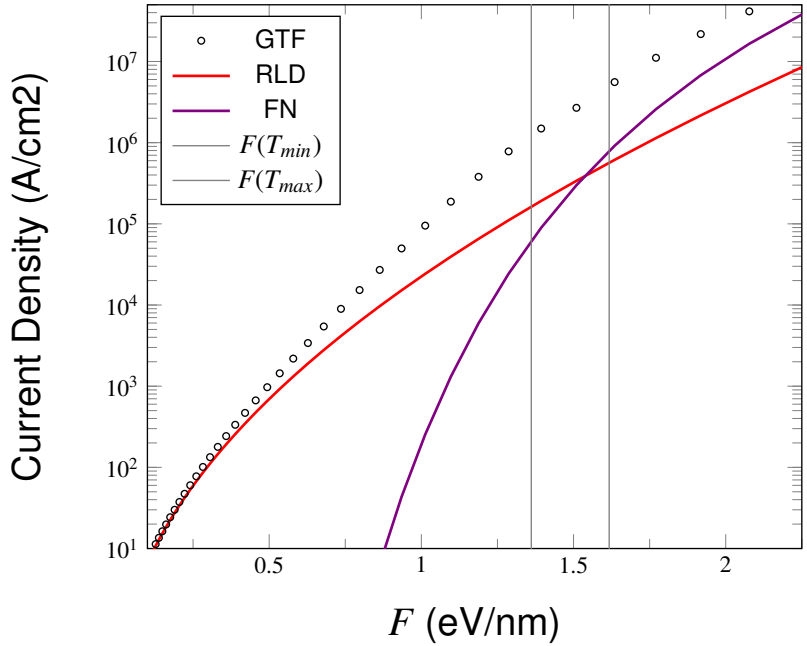

Conventional:
$J_{GTF}(F,T)$ [A/cm^2] for $T = 1173$ K and $\Phi = 4.5$ eV. Also: RLD = Richardson, FN = Fowler-Nordheim, and gray lines corresponding to $F(T_{min}) = 1.361$ eV/nm and $F(T_{max}) = 2.273$ eV/nm as per Eq. (20)

Low Work Function:
$J_{GTF}(F,T)$ [A/cm^2] for $T = 1173$ K and $\Phi = 2.1$ eV. Also: RLD = Richardson, FN = Fowler-Nordheim, and gray lines corresponding to $F(T_{min}) = 1.36$ eV/nm and $F(T_{max}) = 1.617$ eV/nm as per Eq. (20)

Sections Outline

Reformulation Methods

oGTF:[a]

- Three regimes separated by T_{max}, T_{min} in Eq. (20); $\beta_F(E)$ evaluated only at $\beta_F(\mu)$ and $\beta_F(\mu+\phi)$; $v(y)$ and $t(y)$ used;
- $T > T_{max}, n \leq 1 \leftrightarrow$ T-regime;
  $T < T_{min}, n \geq 1 \leftrightarrow$ F-regime
  $T_{min} \leq T \leq T_{max}, n = 1 \leftrightarrow$ TF

rGTF: [b, c]

- Schottky $v(y), t(y)$ no longer used: Shape Factors $\sigma(E), u(E)$ are always used to find $\theta(E), \beta_F(E)$
- E_m is always found exactly $\theta(E)$ always linearized about E_m

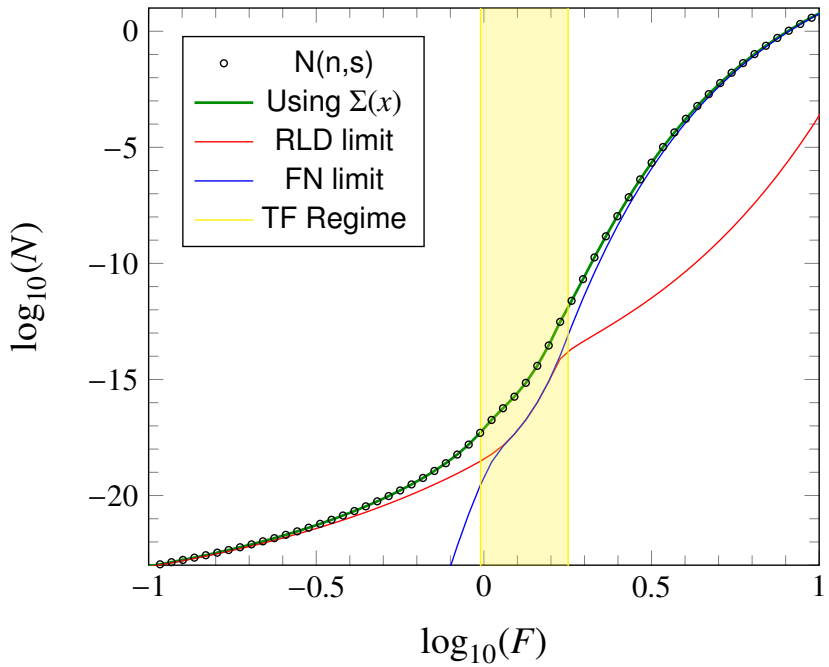

Redefined Regimes

- $n < 0.95 \leftrightarrow$ T-regime
- $n > 1.05 \leftrightarrow$ F-regime
- $|n-1| \leq 0.05 \leftrightarrow$ TF-regime

[a] K.L. Jensen, M. McDonald, O. Chubenko, J.R. Harris, D.A. Shiffler, N.A. Moody, J.J. Petillo, A.J. Jensen, Thermal-field and photoemission from meso- and micro-scale features: Effects of screening and roughness on characterization and simulation. J. Appl. Phys. **125**, 234303 (2019)

[b] K.L. Jensen; A reformulated general thermal-field emission equation J. Appl. Phys. **126**, 065302 (2019).

[c] K.L. Jensen, M. McDonald, J.R. Harris, D.A. Shiffler, M. Cahay, J.J. Petillo; Analytic model of a compound thermal-field emitter and its performance, J. Appl. Phys. **126**, 245301 (2019)

Shape Factor Method I

$\sigma(E)$ and $u(E)$ (related to $\partial_E\theta$) defined by

$$\sigma(E) = \int_{x_-}^{x_+} \left\{ \frac{U(x) - E}{U_o - E} \right\}^{1/2} \frac{dx}{L} \tag{26}$$

$$u(E) = \int_{x_-}^{x_+} \left\{ \frac{U_o - E}{U(x) - E} \right\}^{1/2} \frac{dx}{L} \tag{27}$$

Length/Height scales: ($\phi = \Phi - \sqrt{4QF}$)

$$FL(E) = \sqrt{(\mu + \Phi - E)^2 - 4QF}$$
$$\hbar\kappa(E) \equiv \sqrt{2m(\mu + \phi - E)} \tag{28}$$

Gamow factor using Shape Function

$$\theta(E) = 2\sigma(E)\kappa(E)L(E) \tag{29}$$

$\sigma(E)$ is factor accounting for shape

- rectangular: $\sigma_\square = 1$
- triangular: $\sigma_\triangle = 2/3 = 0.6667$
- parabolic: $\sigma_\cap = \pi/4 = 0.7854$

$\sigma(E)$ = red / blue; $\mu = 7$ eV, $\Phi = 2$ eV, $F = 1$ eV/nm

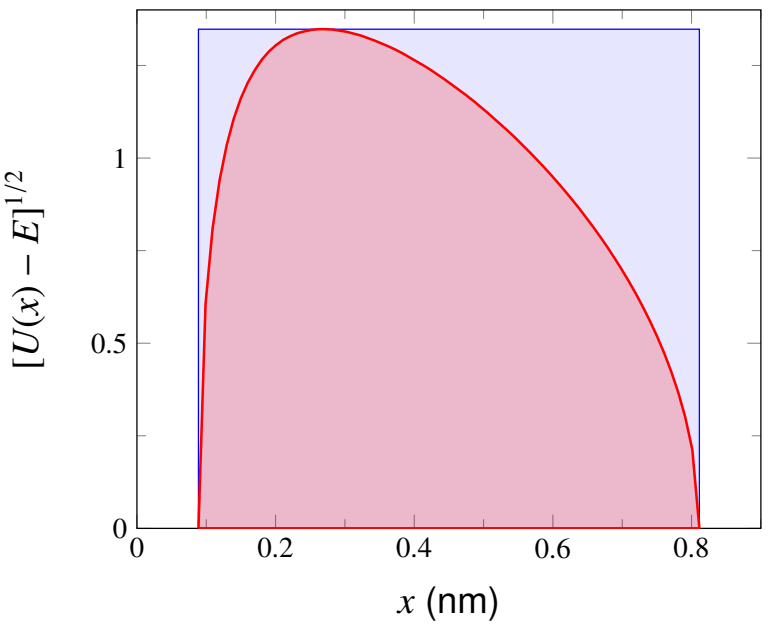

Effect on Fowler-Nordheim Equation

$$J_{FN}(F, \Phi) = \frac{qm}{2\pi^2\hbar^3} \frac{e^{-2\sigma(\mu)\kappa(\mu)L(\mu)}}{[2u(\mu)\kappa(\mu)L(\mu)]^2}$$

$$\sigma(\mu) = \frac{2v(y)}{3(1-y)\sqrt{1+y}}; \qquad u(\mu) = \frac{2t(y)}{\sqrt{1+y}}$$

Shape Factor Method II

oGTF relies on Schottky $v(y)$ and $t(y)$, therefore only for image charge barriers
This is a limitation both theoretically and computationally. Remove them

- $\sigma(E) \to \sigma[y(E)]$
- $y(E) = \dfrac{\sqrt{4FQ}}{\mu + \Phi - E}$
- $U(x)$ between $\triangle$ and $\cap$: $\sigma(y)$ will depend on F or $2/3 < \sigma(y) < \pi/4$

rGTF Eq now uses

$$\theta(E) = 2\,\sigma[y(E)]\,\kappa(E)\,L(E) \tag{30}$$

$$\beta_F(E) = -2\sigma\,\partial_E(\kappa L) - \frac{\kappa L}{\sqrt{QF}}\,y^2\,\partial_y\sigma \tag{31}$$

$$= 2\frac{m^{1/2}Q^{1/4}}{\hbar F^{3/4}}\left[\frac{(y+3)\sigma - 2y(1-y^2)\sigma'}{\sqrt{y(1+y)}}\right]$$

Recover known limits:

FN Limit $y \to 0$ made by $Q \to 0$ (image charge vanishes):

$$\lim_{Q\to 0}\beta_F(E) = \frac{2\sqrt{2m}}{\hbar F}(\mu+\Phi-E)^{1/2}$$

which for $E = \mu$ reproduces FN $\triangle$ result and is "F-like".

RLD Limit $y \to 1$ ($E \to \mu + \phi$):

$$\lim_{y\to 1}\beta_F(E) = \frac{\pi(2m)^{1/2}Q^{1/4}}{\hbar F^{3/4}}$$

reproduces parabolic barrier: "T-like" because $E_m \approx \mu + \phi$ when T high and $F \to 0$.

Shape Factor Method III

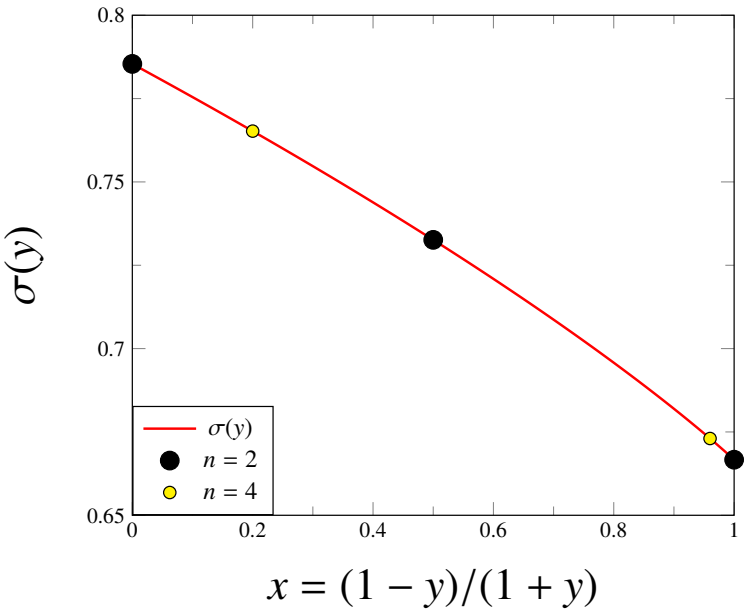

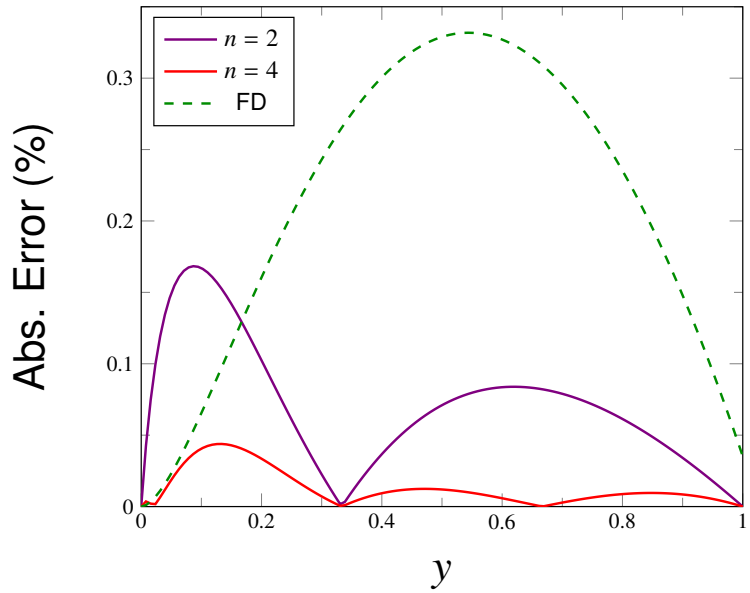

$$\sigma[y(E)] = \sum_{n=1}^{N} C_n \, x(y)^n \qquad (32)$$

j	x_j	y_j	$\sigma(y_j)$
0	0	1	$\pi/4$
1	1/5	2/3	0.76524
2	1/2	1/3	0.73262
3	24/25	1/49	0.67303
4	1	0	2/3

- Error for quadratic & quartic fits.
- Max error is 0.168% and 0.044%, respectively. For comparison, $\sigma(y)$ using Forbes-Deane (FD) approx for $v(y)$ also shown, which is not exact at $y = 1$
- Schottky factors no longer needed in the more general Shape Factor approach, but more importantly, method provides means to correct errors of oGTF in TF-regime

Maximum (Em) Evaluation I

$N(n,s)$ is approximation to "exact" $N[\theta(E)]$:

$$N[\theta(E)] \equiv \beta_T \int_0^\infty \frac{\ln\left(1+e^{\beta_T(\mu-E)}\right)}{1+e^{\theta(E)}} dE \quad (33)$$

- When $\theta(E)$ approximated by linearized Gamow factor, then $\theta(E) \rightarrow \theta_{ns}(E)$ and $N(n,s) = N[\theta_{ns}(E)]$.
- Let $h(E) = N[\theta(E)]$-integrand, so $E_m = \max[h(E)]$
- In T regime, $E_m \approx \mu + \phi$
  In F regime $E_m \approx \mu$
  In TF regime, $\beta_T = \beta_F(E_m)$

Iterative approach to find E_m (iteration labeled by j) is now possible in steps such that $E_m \approx E_5$ typically to 4^{th} decimal place

1. $j = 1$: Let $E_1 = \mu + (1-\epsilon)\phi$ where $\epsilon = 0$ if $\beta_T < \beta_F(\mu+\phi)$, $\epsilon = 1$ if $\beta_T > \beta_F(\mu)$, and otherwise:

$$\epsilon = \frac{2C}{B + \sqrt{B^2 + 4AC}}$$

$$A = 3\left[\beta_F(\mu) + \beta_F(\mu+\Phi)\right] - \frac{6\theta(\mu)}{\phi}$$

$$B = -2\left[\beta_F(\mu) + 2\beta_F(\mu+\Phi)\right] + \frac{6\theta(\mu)}{\phi}$$

$$C = \beta_T - \beta_F(\mu+\phi)$$

2. Obtain $(j+1)^{th}$ estimate from j^{th} by

$$E_{j+1} = E_j - \frac{\Delta}{2}\left(\frac{h_1 - h_{-1}}{h_1 - 2h_0 + h_{-1}}\right)$$

$$h_p \equiv \frac{\ln\left\{1+\exp[\beta_T(\mu - E_j - p\Delta)]\right\}}{1+\exp\left[\theta(E_j + p\Delta]\right)}$$

where $\Delta \approx 0.01$ eV

Maximum (Em) Evaluation II

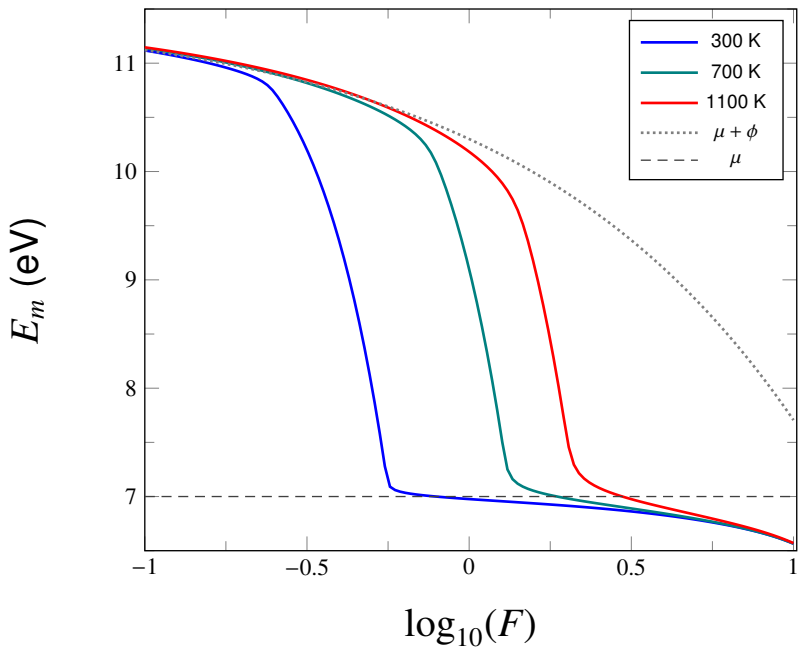

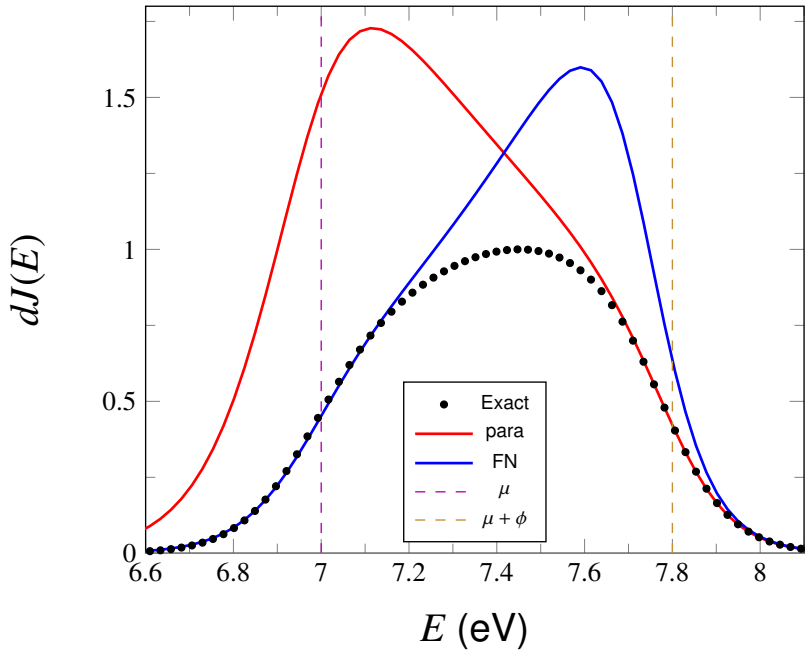

- E_m for various T with $\mu = 7$ eV, $\Phi = 4.5$ eV.
- TF-regime is where E_m departs $\mu + \phi$ line (thermal-like) and converges with μ line (field-like), where oGTF overestimates $dJ(E)$ extent (*left*)
- Observe low T (FN emission) is also overestimated because $\beta_F(E_m) > \beta_F(\mu)$

$dJ(E)$ current integrand for the parameters: $T = 850$ K, $F = 1$ eV/nm, $\mu = 7$ eV, $\Phi = 2$ eV. Gray lines mark $\theta = 0$ (horizontal) and $E = \mu$ and $E = \mu + \phi$ (vertical).

Maximum (Em) Evaluation III

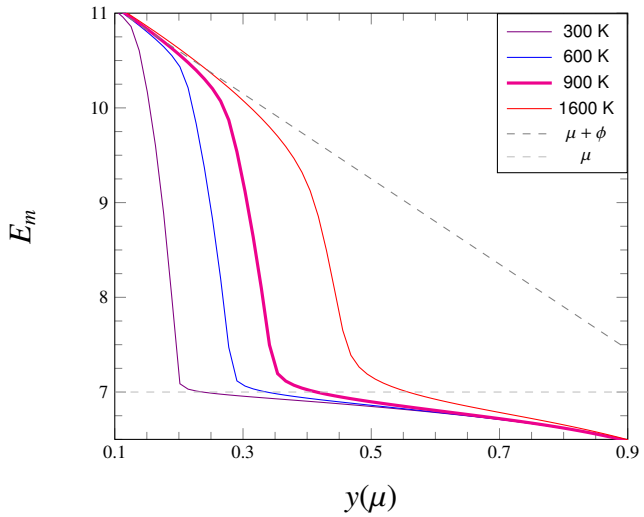

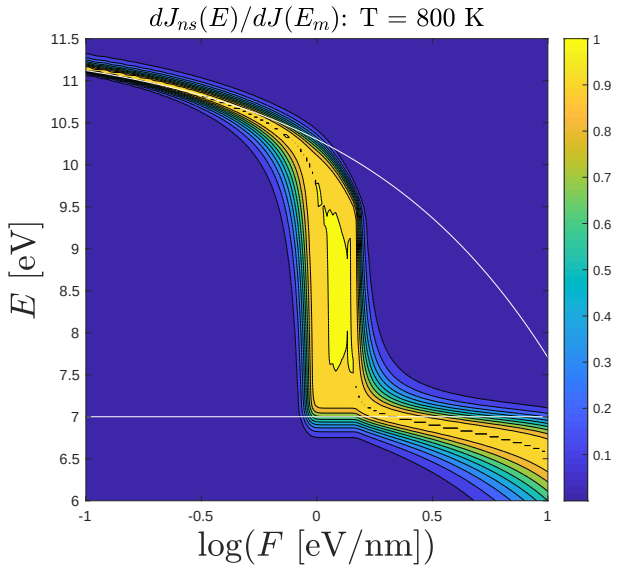

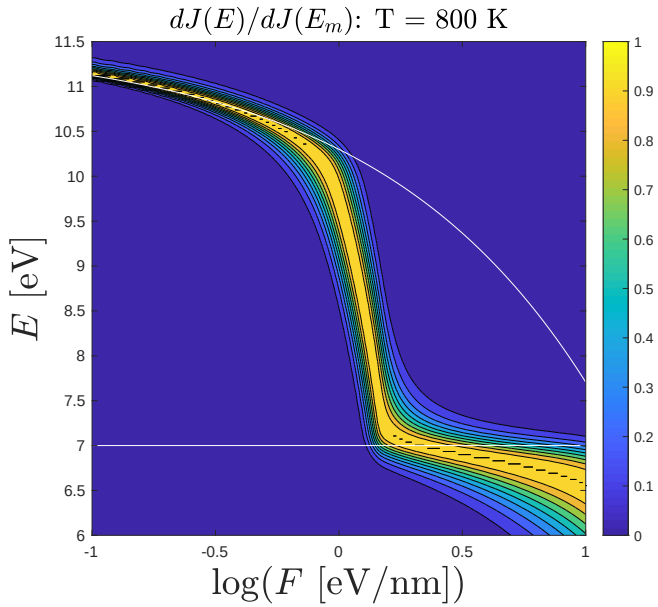

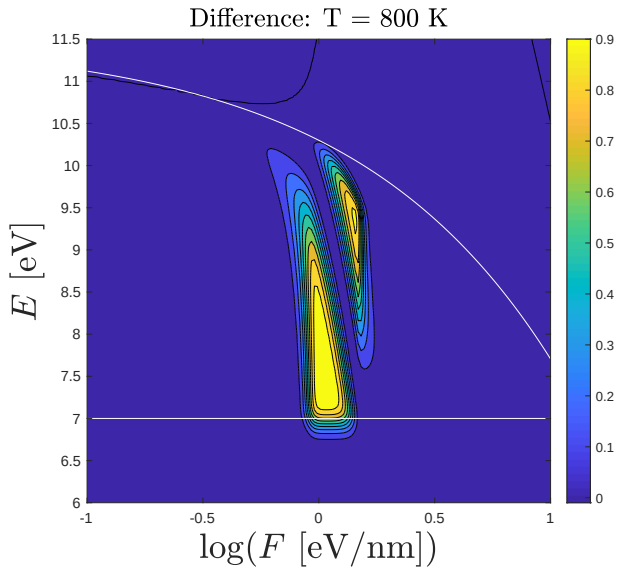

Maximum (Em) Evaluation IV

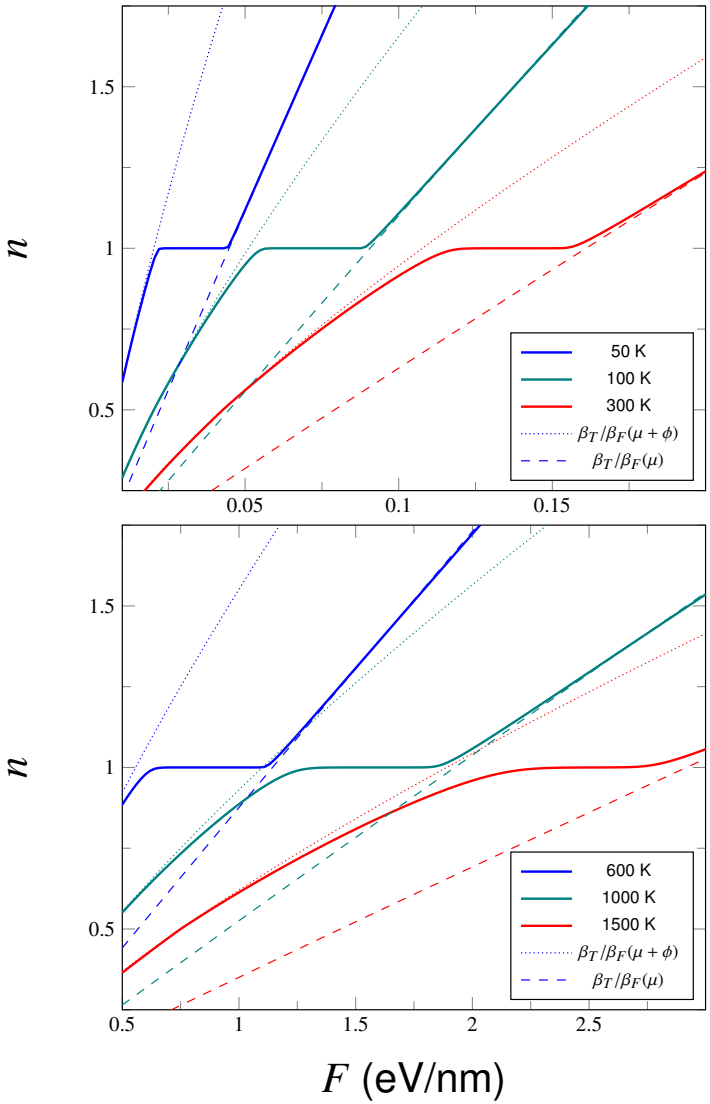

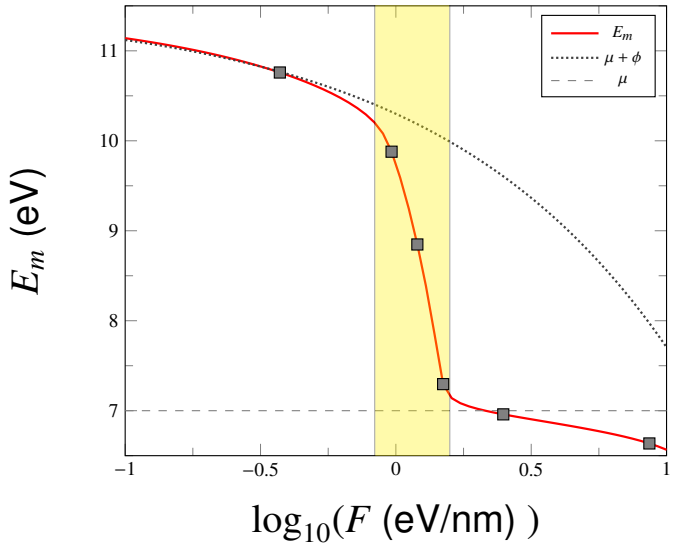

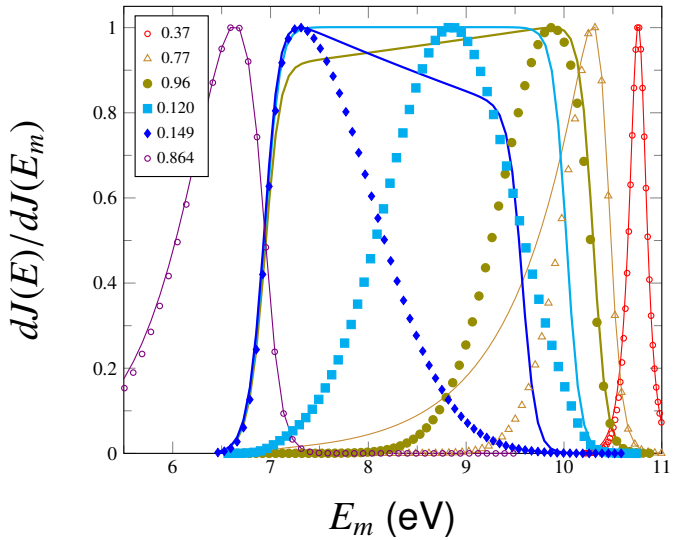

Lorentzian Renormalization Factor I

Ratio Function:

$$R_\theta \equiv \frac{N(n,s)}{N[\theta(E)]} \tag{34}$$

- Lorentzian-like peaks. Enables fast method for finding R_θ. Lorentzians are $L(x) = 1/(x^2+1)$
- Image $L(x)$ makes $R_\theta(0) = 1$; Small y region suppressed via $\Theta(x)$ and

$$\mathbf{L}(y;l,\delta) \equiv L\left(\frac{y-l}{\delta}\right) - L\left(\frac{y+l}{\delta}\right) \tag{35}$$

$$\Theta_\gamma(x) = \frac{1}{2}\left[1 + \tanh\left(\frac{\gamma x}{2}\right)\right] \tag{36}$$

- Fit based on $\sum$ of Lorentzians: $3N+1$ parameters to specify for Eq. (37): C_j, l_j, δ_j, y_w. $N = 4$.

$$R_\theta(y) \approx 1 + \Theta_\gamma(y - y_w)\sum_{j=1}^{N} C_j \mathbf{L}(y; l_j, \delta_j) \tag{37}$$

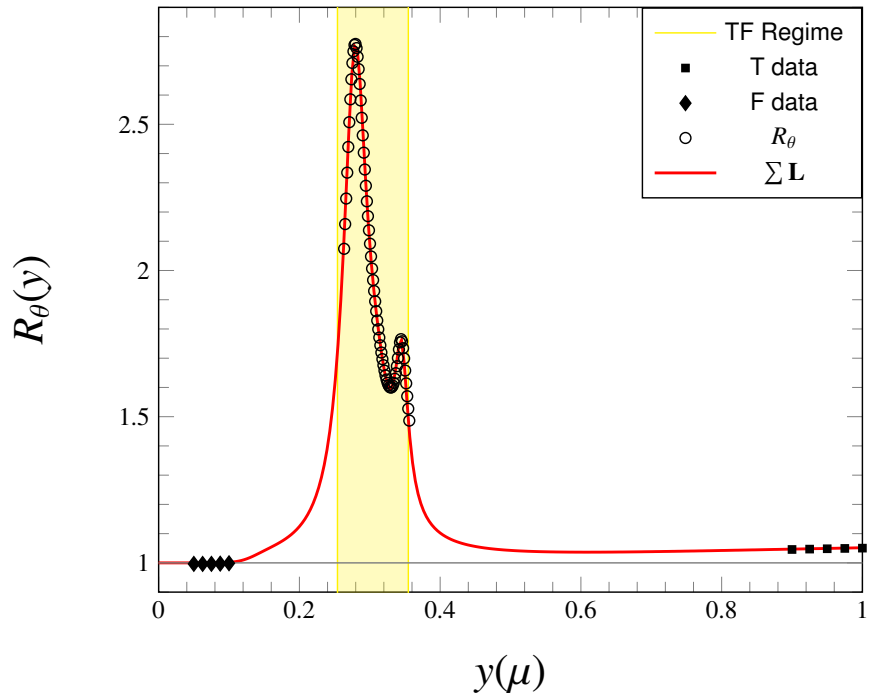

$T = 900$ K, $\Phi = 4.5$ eV. ($\diamond, \circ, \square$); red line is Eq. (37), gray is 1. "F data" used for high field Lorentzian; "T data" identifies where Θ imposed. TF is where $|n-1| \leq 0.05$

Lorentzian Renormalization Factor II

C_j, l_j, δ_j for $T = 900$ K and $\Phi = 4.5$ eV. Observe size of δ_4 necessitates Θ_γ window function

j	C_j	l_j	δ_j
1	1.6484	0.2793	0.0207
2	0.5159	0.3451	0.0116
3	0.2659	0.3101	0.0240
4	0.0643	1.2752	0.8283

top Fitted Lorentzians as per Eq. (37) for pair of parameters (Φ/T) shown in legend. Dotted uses table values

bottom Lorentzians shifted by l_1, normalized by $\max(R_\theta(l_1))$. Analogous underlying behavior (with small variation): suggests possibility of generic parameters C_j, l_j, δ_j, y_w

$R_\theta(y)$ allows $N(n,s)$ via rGTF to be rapidly calculated: useful for characterization, modeling J over single emitter, beam simulations codes, etc. (accommodates $N(n,s)$ - Eq. (16))

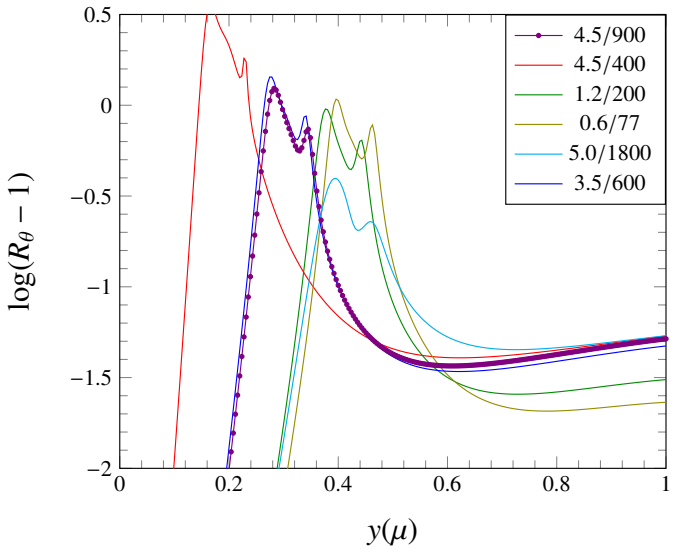

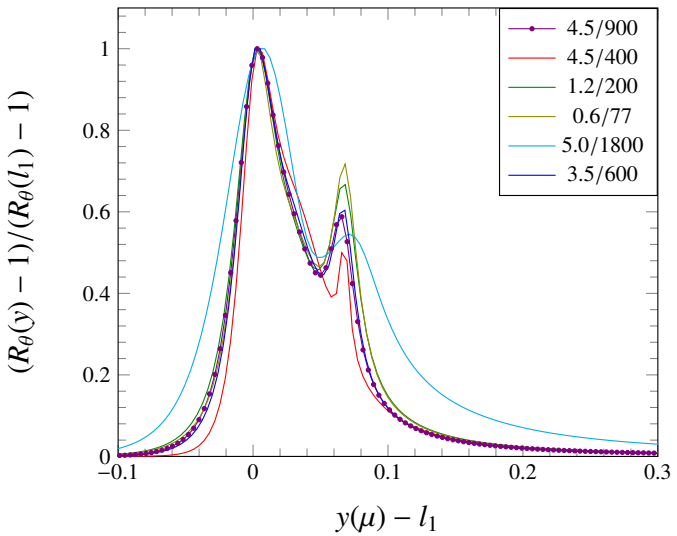

Sections Outline

Compound Emitter I

Characterizing current as thermal-like (RLD) or field-like (FN) is precarious when microscale features exist on mesocale emitters

- For simplicity: on axis protrusion (but methodology allows it anywhere on surface)
- Form compound emitter by placing small dipole atop larger. Dipole potential oriented at polar θ_o wrt $\hat{z}$-axis is given by

$$U_{dip} = \frac{P\,(z\cos\theta_o + \rho\sin\theta_o - a)}{[(z - a\cos\theta_o)^2 + (\rho - a\sin\theta_o]^{3/2}}$$

- P is dipole strength. For primary dipole oriented normal to cathode plane, immersed in background field F_o is $U(\rho, z) = -F_o z + U_{dip}(\rho, z)$ with $\theta_o \to 0$: $U(a\sin\theta, a\sin\theta) \equiv 0 \to P = F_o a^3$ and

$$U(\rho, z) = -F_o z\left[1 - \left(\frac{a^2}{z^2 + \rho^2}\right)^{3/2}\right] \qquad (38)$$
$$\equiv -F_o z + U_o(\rho, z)$$

- Compound emitter: smaller protrusion dipole of strength $\delta P = p(r)F_o a^3$ and radius ra at apex of primary + its image

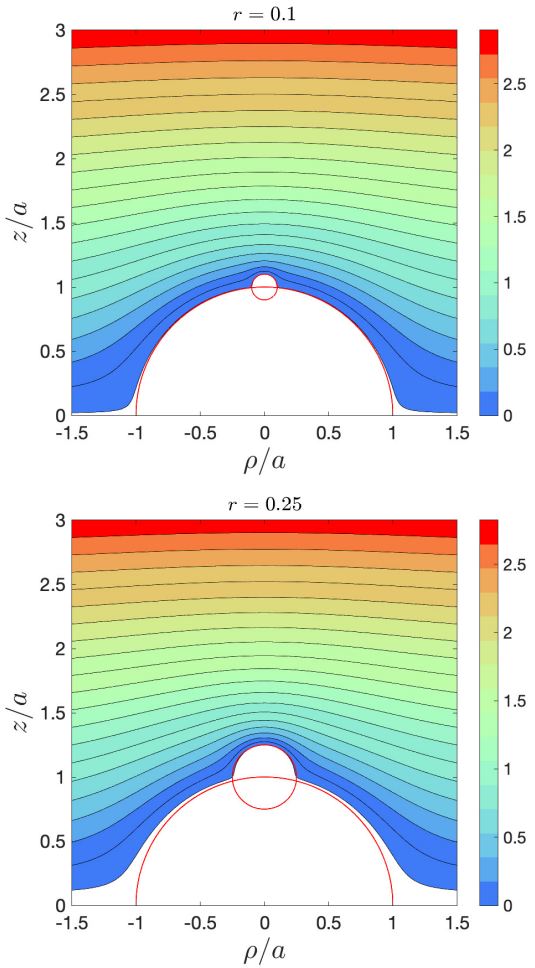

Effective emitter shape shown by white region; red lines are contours of bare single dipole (primary) with same dipole strength.

Compound Emitter II

- Resulting equipotential not contiguous for $U = 0$ surface: made so with inclusion of small background term U_c
- $U(\rho, z)$ vanishes at apex $z_{tip} = (1 + r)a$: sets $p(r)$

$$p = \frac{r + (1 + r^2)^{-3/2} - (1 + r)^{-2}}{r^{-2} + 2(4 + r^2)^{-3/2} - (2 + r)^{-2}} \approx \frac{3}{2} r^3 (2 - 3r) \tag{39}$$

- Choice of U_c satisfies $U(ra, a) = 0$:

$$\frac{U_c}{F_o a} = 1 - \frac{1}{(1 + r^2)^{3/2}} + \frac{2p}{(4 + r^2)^{3/2}} \approx \frac{3}{4} r^2 (2 + r) \tag{40}$$

- Exact forms for computation; approximate forms suggest scaling[a]

[a] K.L. Jensen, M. McDonald, J.R. Harris, D.A. Shiffler, M. Cahay, J.J. Petillo, *Analytic model of a compound thermal-field emitter and its performance*, JAP126, 245301 (2019)

Field Enhancement: Field F_s along (and normal) to surface

$$F_s(\rho) \equiv \sqrt{F_\rho[\rho, z_s(\rho)]^2 + F_z[\rho, z_s(\rho)]^2} \tag{41}$$

Let: $x = \rho/a$, $y = z_s(\rho)/a$, $f_x = F_\rho[\rho, z_s(\rho)]/F_o$ and $f_y = \{F_z[\rho, z_s(\rho)] - F_o\}/F_o$, $\nu = (0, \pm 1)$:

$$f_x = \frac{3xy_0}{R_0} - 3p\left(\frac{xy_+}{R_+} - \frac{xy_-}{R_-}\right)$$
$$f_y = -\frac{x^2 - 2y_0^2}{R_0} + p\left(\frac{x^2 - 2y_+^2}{R_+} - \frac{x^2 - 2y_-^2}{R_-}\right) \tag{42}$$
$$R_\nu = \left[x^2 + y_\nu^2\right]^{5/2}; \quad y_\nu = y + \nu$$

Schottky's conjecture: $\beta_{tip} = F_s/F_o =$ primary $\beta \times$ protrusion β (or $3 \times 3 = 9$)
Analytic (Padé form suggests behavior):

$$\frac{F_{tip}}{F_o} = 1 + \frac{2p}{r^3} + \frac{2}{(1 + r)^3} - \frac{2p}{(2 + r)^3} \approx \frac{9 - 11.56r + 4.273r^2}{1 + 0.3783r - 1.029r^2} \tag{43}$$

departure from $\beta_{tip} = 9$ as r increases faster than anticipated were protrusions to exhibit "self-similarity" (PCM)

Total Current I

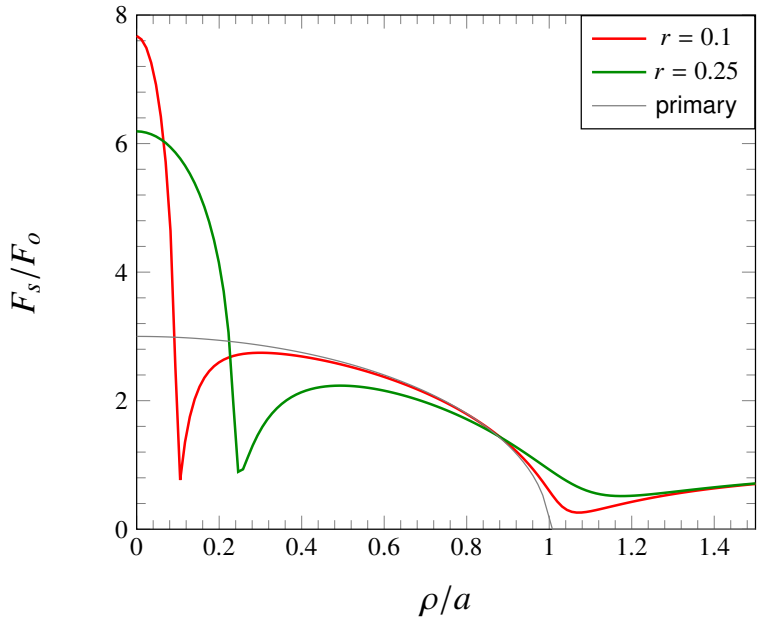

$\beta(\rho) = F[\rho, z_s(\rho)]/F_o$ along surface for $r = 0.1$ and $r = 0.25$; gray line is $\beta(\rho)$ associated with a hemisphere.

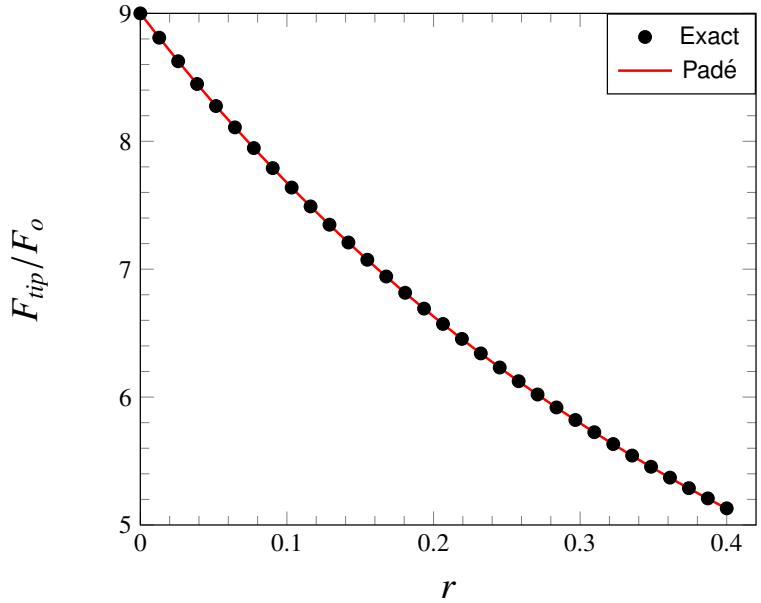

Schottky's conjecture: $\beta_{tip} = F_s/F_o$ = primary $\beta \times$ protrusion β (or $3 \times 3 = 9$): Departure from $\beta_{tip} = 9$ as r increases faster than for "self-similarity" PCM

$$I(V) \equiv \int_{\Omega} J_{GTF}(F_s, T) \sqrt{1 + (\partial_\rho z_s)^2}\, 2\pi\rho\, d\rho \tag{44}$$

Total Current II

Tip current I is J integrated over surface Ω

$$I(V) \equiv \int_{\Omega} J_{GTF}(F_s, T)\, dA \tag{45}$$

$$dA = \sqrt{1 + (\partial_\rho z_s)^2}\, 2\pi\rho\, d\rho \tag{46}$$

e.g., primary emitter: $z_s(\rho) = \sqrt{a^2 - \rho^2}$ and $\rho = a \sin\theta$, then $1 + (\partial_\rho z_s)^2 = \sec^2\theta$ and $dA_h/d\rho = 2\pi a \tan\theta$

Discretize:

$$\partial_\rho z_s \approx \frac{z_s(\rho_{j+1}) - z_s(\rho_j)}{\rho_{j+1} - \rho_j}$$

Discrete surface element:

$$\Delta A_j = \sum_{j=1}^{N} 2\pi\rho_j \sqrt{(\rho_j - \rho_{j-1})^2 + (z_j - z_{j-1})^2} \tag{47}$$

where $\rho_0 = 0$ and $z_0 = (1 + r)a$. $\sqrt{\ldots}$ term is dl_j of ribbon: Average J along ribbon is

$$\left\langle J_j \right\rangle \equiv \frac{1}{2}\left\{J[F_s(\rho_j)] + J[F_s(\rho_{j-1})]\right\} \tag{48}$$

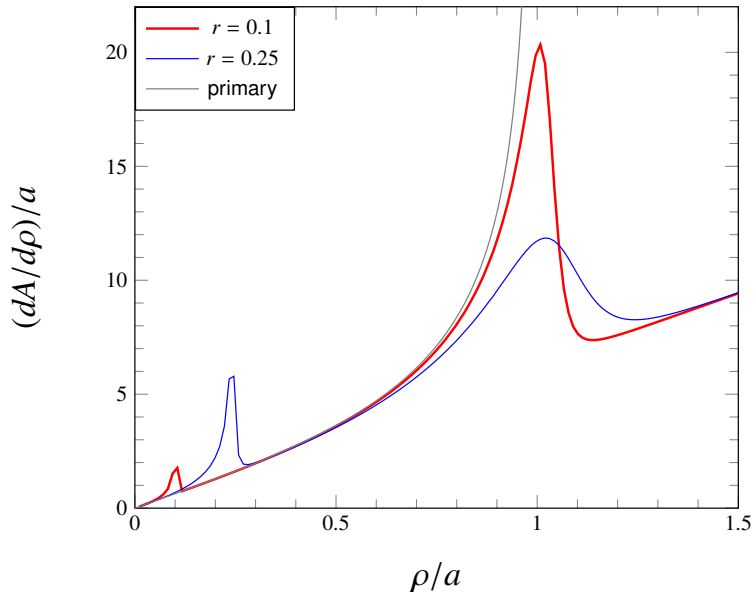

Numerical I(V) From Emitter: $U(D, 0) = qV_a$

$$I(V_a) = \sum_{j=1}^{N} \left\langle J_j \right\rangle \Delta A_j \tag{49}$$

Limiting cases

$$I_t(V_a) = 2\pi a^2 \int_0^1 J_{RLD}(T, 3F_o x)\, dx \tag{50}$$

$$I_f(V_a) = 2\pi (ra)^2 \int_0^1 J_{FN}(\beta_{tip} F_o x)\, dx \tag{51}$$

Characterization I

- Departures of $J(F)$ from J_t and J_f reveal the onset of TF emission[a]
- Departures of $I(V)$ from I_t and I_f reveal how compound emitter transitions from being a thermal emitter at low fields to being a field emitter at high fields
- Intermediate field regime poorly characterized by such a dichotomy: T-dominated processes (on primary) co-exist with F-dominated processes (on protrusion) on same compound structure
- Comparison for $r = (0.1, 0.25) = (\circ, \bullet)$
  I_f (dark / light) blue for $(\circ, \bullet)$
  I_t (in red) due to primary
- Factor of $5/4$ associated with base for I_t brings RLD agreement with GTF at low F.

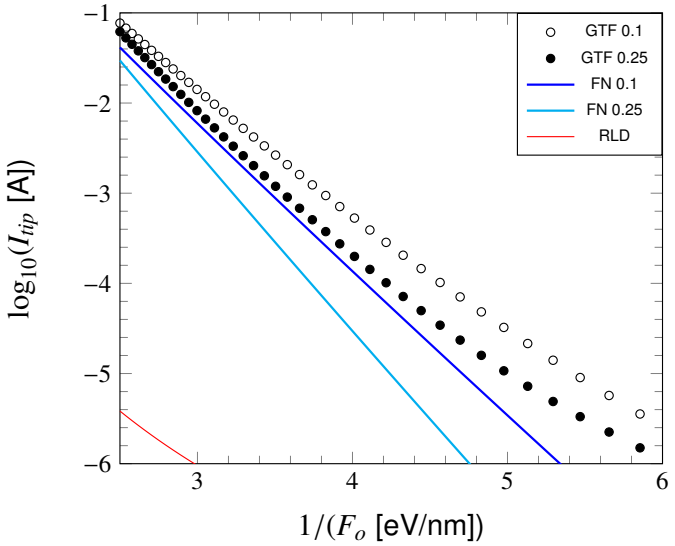

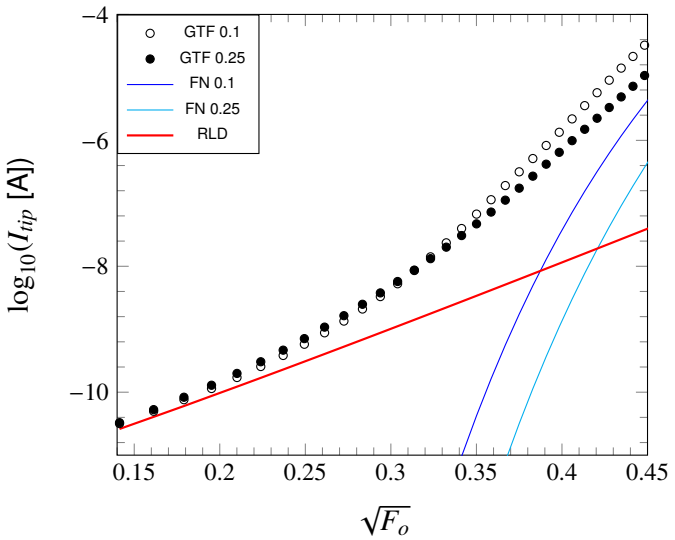

[a] K.L. Jensen, M. McDonald, J.R. Harris, D.A. Shiffler, M. Cahay, J.J. Petillo, *Analytic model of a compound thermal-field emitter and its performance* JAP126, 245301 (2019)

Characterization II

- fit[a] to $\ln(I/F_o^2) = Y - S/F_o$
- infer β, A_o

$$\beta = \frac{4v_o\sqrt{2m\Phi^3}}{3\hbar S}$$

$$A_o = \frac{e^Y}{A_{sp}\beta^2}$$

- Numerical: $r = 0.10$,
  $\beta = 7.68, 8411 < A(F_o) < 9762$
  YS: $\beta = 9.21$ and $A_o = 907$ nm^2
- Numerical: $r = 0.25$,
  $\beta = 6.19, 59383 < A(F_o) < 50455$
  YS: $\beta = 8.13$ and $A_o = 1912$ nm^2
- β over by $20\% - 30\%$,
  A_o under by $10 - 30\times$

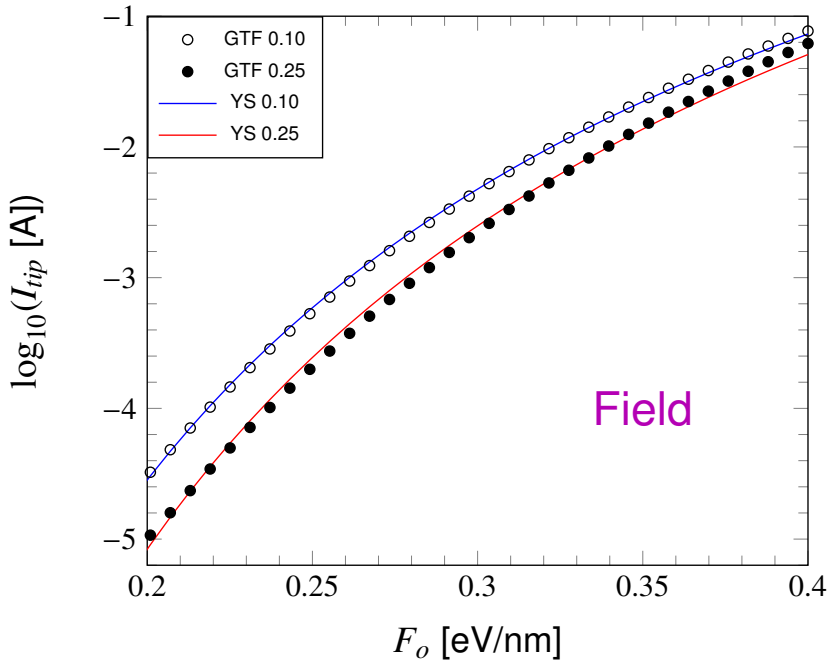

Fowler-Nordheim
using Spindt $v(y), t(y)$ (sp):

$$I(F_o) = A_o J_{sp}(F_o)$$

[a] all units in (eV, nm, fs, q)

Characterization III

- Calibrate

$$\beta_{eff} = \frac{(k_B T)^2}{4Q}\left[\frac{\ln(I_a/I_b)}{\sqrt{F_a} - \sqrt{F_b}}\right]^2$$

- fit[a] to $\ln(I/T^2) = Y - S/T$

$$\Phi_{eff} = k_B S + \sqrt{4\beta_{eff} F_o Q}$$

$$A_{eff} = \frac{e^Y}{A_{RLD}}$$

- Numerical: $\beta = 3, \Phi = 2.6$ eV, $A/\pi a^2 = 1 + r^2 + (9/4)$
- YS (0.10): $\beta = 2.12, \Phi = 2.26, A/\pi a^2 = 0.443$
  YS (0.25): $\beta = 2.38, \Phi = 2.27, A/\pi a^2 = 0.425$

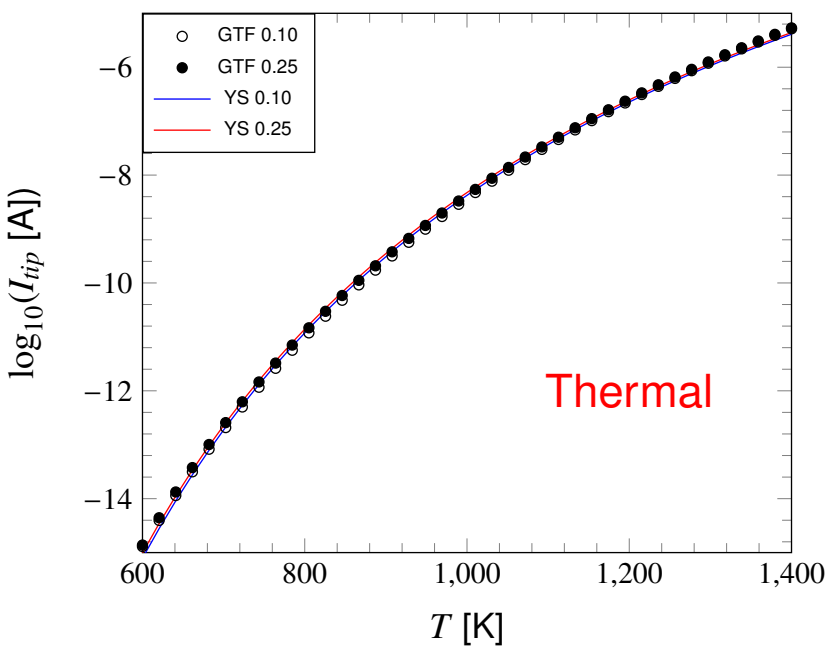

Richardson Eq.

$$I_{RLD}(F_o) = A_c J_{RLD}(T)$$

[a] all units in (eV, nm, fs, q)

Concluding Remarks

Reformulated General Thermal Field Emission

- Designed for rapid and repeated evaluation of emission from mesoscale structures with microscale protrusions
- ...to meet the needs of interpreting characterization measurements, prediction of performance from compound emitters, and providing models that can profitably be used in the simulation of electron beams
- Lorentzian correction accounts for departures of $\theta(E)$ from its linear approximation

Impact On Usage and Characterization

- Compound emitter is a combination of point dipoles describing the primary base and the apex protrusion and is analytic
- rGTF applied to compound emitter for conditions where T, F, TF emission simultaneously exist and contribute
- rGTF $I(V)$ prediction contrasted to RLD and FN: current vastly underestimated and affects characterization
- Entails consequences on characterization of emitters, simulation in devices using density modulated beams, and particle-in-cell (PIC) codes.